Electron Momentum Spectroscopy of pyrimidine at the benchmark ADC(3) level

ARTICLE *in* CHEMICAL PHYSICS LETTERS · SEPTEMBER 2010

Impact Factor: 1.9 · DOI: 10.1016/j.cplett.2010.08.055

3 AUTHORS, INCLUDING:

Seiyed Hamid Reza Shojaei
Hasselt University
10 PUBLICATIONS **30** CITATIONS
SEE PROFILE

Michael S Deleuze
Hasselt University
132 PUBLICATIONS **2,672** CITATIONS
SEE PROFILE

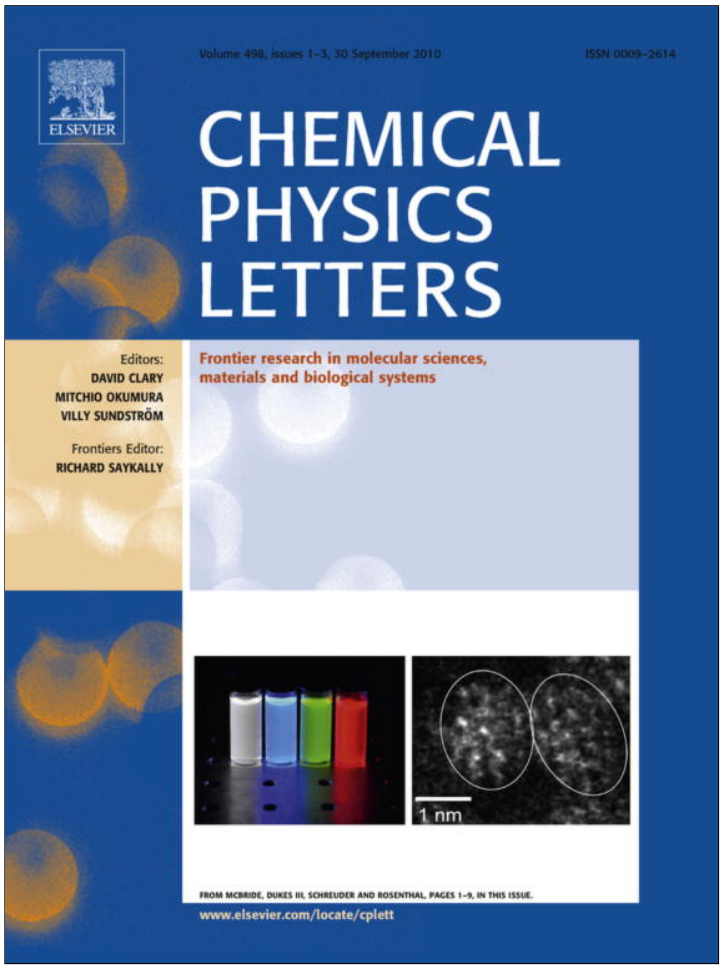

Chemical Physics Letters 498 (2010) 45–51

Contents lists available at ScienceDirect

Chemical Physics Letters

journal homepage: www.elsevier.com/locate/cplett

Electron Momentum Spectroscopy of pyrimidine at the benchmark ADC(3) level

S.H. Reza Shojaei, Bálazs Hajgató, Michael S. Deleuze *

Research Group of Theoretical Chemistry and Molecular Modelling, Hasselt University, Agoralaan Gebouw D, B-3590 Diepenbeek, Belgium

ARTICLE INFO

Article history:
Received 2 July 2010
In final form 23 August 2010
Available online 26 August 2010

ABSTRACT

An extensive study of the valence electronic structure, ionization spectrum and electron momentum distributions of pyrimidine is presented, on the ground of accurate calculations of one-electron and shake-up ionization energies and of the related Dyson orbitals, using one-particle Green's Function theory in conjunction with the third-order Algebraic Diagrammatic Construction scheme [ADC(3)]. Comparison is made with results obtained from standard (B3LYP) Kohn–Sham orbitals and recent measurements employing Electron Momentum Spectroscopy. Quantitative insights into the experimental momentum distributions are amenable without resorting to any empirical rescaling of pole strengths, provided band overlaps and relaxation effects are properly accounted for.

1. Introduction

The main purpose of the present work is to sort out a major contradiction between the results of a recent interpretation [1] of experiments employing Electron Momentum Spectroscopy [2–4] upon pyrimidine, on the ground of empirically rescaled Kohn–Sham momentum distributions, and the results of a theoretical study of the valence shell photoelectron spectrum obtained for this compound using synchrotron radiation [5], at photon energies of 45 and 85 eV, by means of one-particle Green's Function (1p-GF) theory [6–9], along with the third-order Algebraic Diagrammatic Construction [ADC(3)] scheme [9–13].

Despite its rather low energy resolution (0.5 eV, at best [14]), Electron Momentum Spectroscopy (EMS) is known to be a powerful orbital imaging technique, which enables experimental reconstructions of spherically averaged one-electron transition momentum distributions corresponding to specific ionization channels. This usually implies an angular analysis of ionization intensities in binary (e,2e) electron impact ionization experiments ($M + e^- \rightarrow M^+ + 2e^-$) at high kinetic energies and under a non-planar symmetric kinematical set-up. The Born (sudden), binary encounter, plane wave impulse and target Kohn–Sham [15] approximations are traditionally invoked and justify the comparison of experimentally inferred momentum profiles with structure factors derived from the momentum space representation of Kohn–Sham orbitals.

A most common practice with EMS experiments is to rescale the simulated momentum distributions onto experiment in order to empirically account for the flux of ionization intensity towards shake-up and correlation bands at (normally) higher binding energies. In their EMS study of pyrimidine, Ning et al. have thereby inferred an empirical value of 0.80 for the pole strength (Γ) characterizing the $2b_1$ ionization band at a binding energy (ε_b) of 10.5 eV, relative to the $7b_2$ and $\{11a_1 + 1a_2\}$ ionization bands at 9.8 and 11.3 eV, respectively, for which no loss in ionization intensity was assumed ($\Gamma = 1$). This conclusion was found to be at odds with the results of the ADC(3) calculations that were presented in [5]: according to these calculations, the pole strengths characterizing the four outermost ionization lines of pyrimidine are all around ~0.89, which shows that the one-particle picture of ionization prevails for these four lines. If they did not provide any robust enough experimental evidence that the missing (20%) fraction of the $2b_1$ ionization intensity could be found somewhere else in their (e,2e) ionization spectrum, Ning et al. nonetheless ascribed [1] this apparent failure of 1p-GF/ADC(3) theory to limitations in the basis set that was employed in the work by Potts et al. [5], namely Pople's 6–31G basis set [16], which in the past used to be highly popular. They also rather abusively invoked as a further argument a joined and very specific study with our group of a high-lying ($\varepsilon_b \sim 29$ eV) and extremely weak transition ($\Gamma \sim 0.02$) describing the $2a_1$ shake-up ionization onset in the (e,2e) ionization spectrum of water [17]. Because of the extremely pronounced Rydberg character of the involved electronic excitation, the latter band has required a [SAC-CI general-R] theoretical treatment at higher orders in electronic correlation, in order to achieve a highly quantitative match with experiment, within ~0.2 eV accuracy.

Countless studies (see e.g. [18–21]) and references therein) over the last three decades have shown that the 1p-GF/ADC(3) approach enables reliable and accurate studies of one-electron and shake-up ionization energies at the usual HeI (0–21.22 eV) binding energy range, and in general up to those binding energy regions where complete breakdowns of the orbital picture of ionization are observed. In the present work, we shall reassign the available

* Corresponding author. Fax: +32 11 26 83 01.
E-mail address: michael.deleuze@uhasselt.be (M.S. Deleuze).

0009-2614/$ - see front matter © 2010 Elsevier B.V. All rights reserved.
doi:10.1016/j.cplett.2010.08.055

photoelectron and (e,2e) ionization spectra, as well as the related momentum profiles, through a comparison with the results of ADC(3) calculations employing larger basis sets, and this up to electron binding energies of ~33 eV. Quite naturally, the relationships that prevail between 1p-GF and EMS theories [22] will be exploited through a systematic comparison of Kohn–Sham orbital momentum distributions against experiment and intrinsically more reliable ADC(3) Dyson orbital momentum distributions, which explicitly account for configuration interactions in both the initial ground state and the final ionized state.

2. Computational details

All computations that are presented in this work have been carried out upon ground-state geometrical parameters that were optimized under the constraint of the C_{2v} symmetry point group, using Density Functional Theory (DFT [23]) along with the standard hybrid gradient corrected Becke-3-parameter-Lee–Yang-Parr (B3LYP) functional [24], in conjunction with Dunning's aug-cc-pVTZ basis set ([25,26], i.e. correlation consistent polarized valence triple zeta basis set, augmented by sets of diffuse *s*, *p*, *d*, and *f* atomic functions on carbons, and diffuse *s*, *p* and *d* functions on hydrogens.

The ADC(3) calculations have been performed by means of the original code [27] interfaced to the GAMESS package of programs [28], under the assumption of frozen core electrons, using charge-consistent one-electron densities for computing static self-energies with the appropriate size-intensive scaling [29]. The band Lanczos diagonalization approach [30,31] was used for projecting the 2*p*-1*h* shake-on states associated with the electron affinity blocks of the secular matrix to diagonalize onto a pseudo-electron attachment spectrum, prior to completing the diagonalization process, by means of the block-Davidson approach [32]. All eigenstates with pole strength greater than or equal to 0.005 have been recovered up to electron binding energies of 33 eV. At the SCF level, the requested convergence on the elements of the one-electron density matrix was set equal to 10^{-10}.

In reply to the criticisms by Ning et al. [1] onto the work by Potts et al. [5], we shall comparatively assess ADC(3) calculations performed using three basis sets of improving quality: the standard Pople's 6–31G basis set [16], Dunning's correlation consistent polarized valence basis set of double zeta quality (cc-pVDZ [25]) and the so-called cc-pVDZ++ basis set, which incorporates diffuse sets of *s* and *p* functions taken from the aug-cc-pVDZ basis set [25,26] on carbons and hydrogens (severe linear dependencies resulting in numerical divergences in the inversion procedure for evaluating static self-energies [11] prevented us from completing successfully ADC(3) calculations with the latter basis set). Comparison will be made with results of larger scale calculations of one-electron ionization energies employing the Outer-Valence Green's Function approach [8,9].

Theoretical ionization spectra have been constructed by convoluting the ADC(3) results, using as convolution function a Voigt profile combining a Gaussian and a Lorentzian functions with equal weight and a constant full width at half-maximum (FWHM) parameter of 0.6 eV. This convolution takes into account in an average and very approximate way various contributions to line broadening. Whereas the Gaussian component of the Voigt profile takes into account the outcome of the limited experimental resolution in energy, vibrational effects, ... etc., the Lorentzian component especially accounts for the natural line width due to the limited lifetime of ionized states. The chosen band width was taken as a practical compromise between that seen in the PES measurements by Potts et al. (~0.4 eV), on the one hand, and on the other hand the EMS experiments by Ning et al. (~0.9 eV).

In line with the usual prescriptions for analyzing EMS experiments, the Born (sudden), binary encounter and plane wave impulse approximations are invoked for simulating (e,2e) electron momentum distributions obtained using a standard (e,2e) non-coplanar symmetric kinematical set-up at an electron impact energy of 1.5 keV. The B3LYP Kohn–Sham momentum distributions have been computed in conjunction with Dunning's correlation consistent polarized valence basis sets of double zeta quality augmented by a set of *s*, *p*, *d* (*s*, *p*) diffuse functions on carbons (hydrogens) (aug-cc-pVDZ basis set [25,26]), as well as with the closely related cc-pVDZ++ basis set. Dyson orbital momentum distributions have been correspondingly computed at the ADC(3)/cc-pVDZ++ level.

Spherically averaged orbital momentum distributions have been generated from the output of 1p-GF/ADC(3) or DFT calculations using the MOMAP program by Brion and co-workers [33]

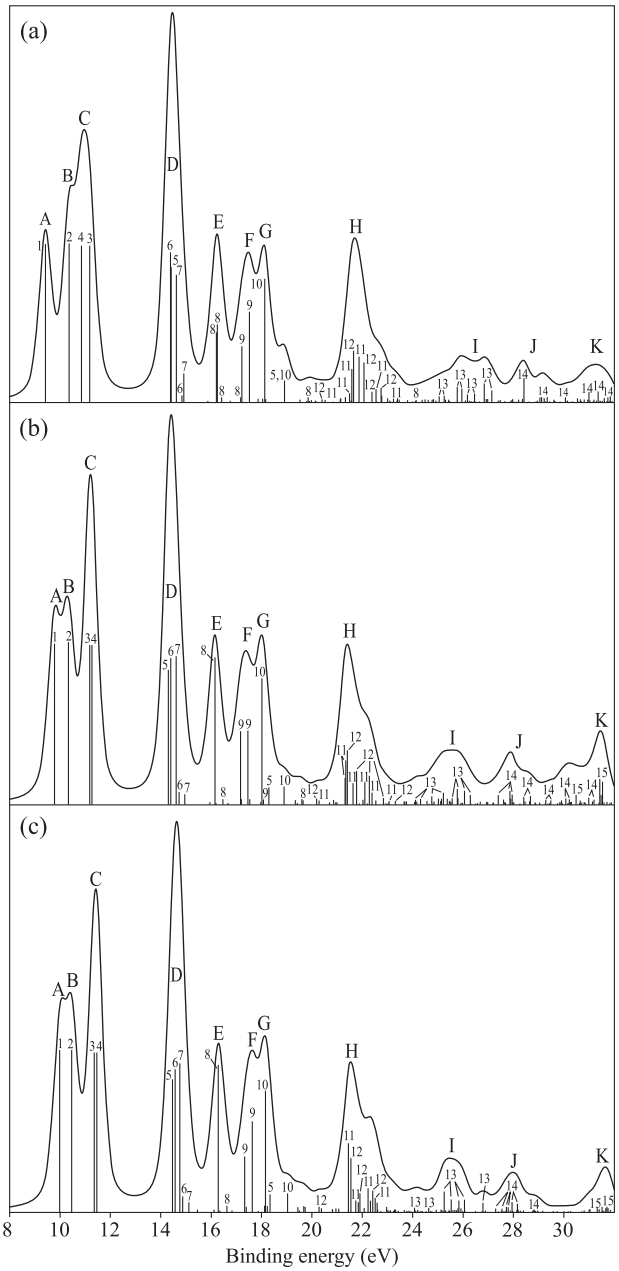

Figure 1. Theoretical ADC(3) ionization spectra of pyrimidine ($C_4N_2H_4$, C_{2v} symmetry point group) obtained using the (a) 6-31G, (b) cc-pVDZ and (c) cc-pVDZ++ basis sets. See Table 1 for a detailed assignment of lines and bands.

Table 1
ADC(3) and OVGF calculations of the ionization spectrum of pyrimidine. Binding energies are given in eV, along with spectroscopic factors (in parentheses)[a].

Label	M.O.[(1)]	KT/cc-pVDZ++	ADC(3)/6-31G		ADC(3)/cc-pVDZ		ADC(3)/cc-pVDZ++		OVGF/cc-pVDZ		OVGF/aug-cc-pVTZ		PES[5]	EMS[1]
1	$7b_2$ (n)	11.341	9.431	(0.896)	9.774	(0.890)	9.991	(0.888)	9.505	(0.899)	9.880	(0.893)	9.8	9.8
2	$2b_1$ (π)	10.354	10.364	(0.898)	10.326	(0.895)	10.473	(0.890)	10.219	(0.906)	10.482	(0.899)	10.5	10.5
3	$1a_2$ (π)	11.570	11.187	(0.883)	11.187	(0.880)	11.364	(0.875)	11.038	(0.895)	11.282	(0.888)	11.2	11.3
4	$11a_1$ (n)	12.934	10.864	(0.886)	11.261	(0.879)	11.471	(0.876)	11.064	(0.894)	11.406	(0.888)	11.5	
5	$1b_1$ (π)	15.797	14.405	(0.763)	14.296	(0.740)	14.463	(0.731)	14.262	(0.832)	14.490	(0.826)	13.9	14.1
			18.037	(0.022)	17.540	(0.032)	17.641	(0.033)						
			18.909	(0.100)	18.291	(0.096)	18.339	(0.099)						
			20.146	(0.011)	19.639	(0.027)	19.730	(0.028)						
6	$10a_1$ (σ)	16.066	14.393	(0.847)	14.398	(0.806)	14.573	(0.784)	14.242	(0.891)	14.522	(0.885)		
			14.839	(0.041)	14.735	(0.069)	14.870	(0.086)						
7	$6b_2$ (σ)	16.300	14.630	(0.720)	14.600	(0.817)	14.759	(0.817)	14.399	(0.892)	14.668	(0.886)	14.4	
			14.919	(0.163)	14.954	(0.058)	15.117	(0.053)						
			16.766	(0.012)	–	(–)	–	(–)						
			19.526	(0.020)	–	(–)	–	(–)						
8	$9a_1$ (σ)	17.800	16.215	(0.396)	16.147	(0.812)	16.287	(0.807)	15.943	(0.880)	16.163	(0.873)	15.8	15.7
			16.260	(0.441)	16.474	(0.032)	16.632	(0.035)						
			16.419	(0.033)	–	(–)	–	(–)						
			17.171	(0.032)	17.206	(0.030)	–	(–)						
			19.851	(0.032)	19.590	(0.034)	19.680	(0.033)						
			24.139	(0.014)	–	(–)	–	(–)						
9	$5b_2$ (σ)	19.214	17.225	(0.318)	17.168	(0.405)	17.332	(0.304)						
			17.525	(0.512)	17.469	(0.408)	17.637	(0.498)	16.895	(0.862)	17.127	(0.853)	17.0	17.5
			17.854	(0.024)	18.078	(0.030)	18.233	(0.034)						
			18.171	(0.022)	19.349	(0.026)	19.448	(0.028)						
10	$8a_1$ (σ)	20.214	18.132	(0.699)	18.014	(0.697)	18.124	(0.036)					17.7	
			18.909	(0.127)	18.888	(0.101)	18.162	(0.665)	17.956	(0.857)	18.182	(0.849)		
			21.142	(0.026)	20.856	(0.027)	19.039	(0.103)						
			–	(–)	22.525	(0.025)	–	(–)						
			–	(–)	23.300	(0.022)	–	(–)						
11	$7a_1$ (σ)	24.400	21.496	(0.054)	20.288	(0.025)	–	(–)						
			21.578	(0.190)	21.314	(0.149)	–	(–)						
			21.584	(0.098)	21.331	(0.242)	20.379	(0.023)						
			21.874	(0.259)	21.623	(0.118)	20.952	(0.022)						
			22.545	(0.077)	22.092	(0.122)	21.447	(0.379)	21.402	(0.815)	21.600	(0.788)		
			22.779	(0.040)	22.380	(0.067)	21.737	(0.064)						
			23.006	(0.025)	24.550	(0.023)	22.221	(0.133)						
			23.236	(0.023)	–	(–)	22.513	(0.079)						
			24.823	(0.020)	–	(–)	22.588	(0.052)						
12	$4b_2$ (σ)	24.504	20.404	(0.020)	20.181	(0.035)	20.280	(0.031)						
			21.126	(0.020)	–	(–)	21.543	(0.295)	21.442	(0.806)[b]	21.628	(0.795)		
			21.327	(0.033)	–	(–)	21.838	(0.054)						
			21.653	(0.292)	21.408	(0.300)	21.899	(0.103)						
			22.066	(0.226)	21.766	(0.186)	22.071	(0.023)						
			22.380	(0.063)	22.016	(0.027)	22.319	(0.061)						
			22.746	(0.085)	22.283	(0.160)	22.415	(0.119)						
			23.401	(0.025)	22.828	(0.039)	22.963	(0.029)						
13	$6a_1$ (σ)	29.434	–	(–)	24.103	(0.028)	24.072	(0.025)	–	(-)				
			–	(–)	24.299	(0.032)	–	(–)						
			–	(–)	24.757	(0.047)	24.637	(0.025)						
			–	(–)	24.835	(0.020)	–	(–)						
			–	(–)	25.000	(0.032)	–	(–)						
			25.057	(0.036)	25.133	(0.034)	–	(–)						
			25.252	(0.039)	25.211	(0.066)	–	(–)						
			25.772	(0.090)	25.374	(0.035)	25.253	(0.114)						
			25.957	(0.080)	25.464	(0.022)	25.534	(0.071)						
			26.180	(0.047)	25.561	(0.037)	25.802	(0.023)						
			26.846	(0.109)	25.767	(0.078)	25.836	(0.064)						
			26.921	(0.020)	25.785	(0.037)	25.919	(0.021)						
			26.977	(0.020)	26.049	(0.077)	26.060	(0.069)						
			27.142	(0.070)	26.272	(0.054)	26.790	(0.053)						
14	$3b_2$ (σ)	32.745	27.975	(0.020)	27.379	(0.051)	27.296	(0.020)						
			28.369	(0.021)	27.599	(0.029)	27.720	(0.030)						
			28.420	(0.138)	27.848	(0.074)	27.790	(0.027)						
			29.055	(0.029)	27.867	(0.024)	27.948	(0.056)						
			29.121	(0.031)	27.894	(0.034)	28.159	(0.046)						
			29.226	(0.024)	27.942	(0.056)								
			29.339	(0.031)	28.389	(0.041)								
			30.066	(0.030)	28.635	(0.020)								
			30.540	(0.023)	28.673	(0.048)								
			31.003	(0.060)	29.275	(0.026)								
			31.371	(0.062)	29.476	(0.023)								

(*continued on next page*)

Table 1 (*continued*)

Label	M.O.[(1)]	KT/cc-pVDZ++	ADC(3)/6-31G		ADC(3)/cc-pVDZ		ADC(3)/cc-pVDZ++		OVGF/cc-pVDZ	OVGF/aug-cc-pVTZ	PES[5]	EMS[1]
			31.614	(0.025)	29.898	(0.022)						
			31.763	(0.030)	30.070	(0.035)						
			31.856	(0.035)	30.209	(0.029)						
					30.980	(0.039)						
15	$5a_1$ (σ)	35.969	31.209	(0.017)	30.476	(0.052)	31.327	(0.023)				
					30.636	(0.024)	31.516	(0.030)				
					31.181	(0.028)	31.652	(0.025)				
					31.417	(0.140)	31.689	(0.024)				
					31.471	(0.054)	31.701	(0.031)				
					31.518	(0.126)	31.722	(0.028)				
							31.754	(0.023)				
							31.768	(0.021)				

[a] Only ionization lines with pole strengths larger than 0.02 are listed.
[b] Breakdown of the MO picture of ionization; see Ref. [44].

and homemade interfaces. In line with the characteristics of the (e,2e) spectrometer that is currently employed at Beijing university [34], our calculations also account for a limited resolution of $\Delta\phi = \pm 0.84^\circ$ and $\Delta\theta = \pm 0.57^\circ$ on the azimuthal and polar angles in the (e,2e) kinematical set up, using a procedure employing Monte Carlo simulations [35] for computing the resolution-folded and spherically averaged (e,2e) electron momentum distributions. In order to account for the stronger dispersion of the ionization intensity towards shake-up structures at higher binding energies, experimental intensities have been rescaled onto our best [ADC(3)/cc-pVDZ++] momentum distributions, using a global factor obtained through a least square fitting of summed experimental (e,2e) intensities onto theoretical (ADC(3)/cc-pVDZ++) intensities for all ionization bands (**A**–**G**) or lines (**1**–**10**) recovered until $\varepsilon_b \sim 19$ eV. For the sake of consistency in the analysis, the Kohn–Sham B3LYP momentum distributions have been correspondingly rescaled by the relevant ADC(3)/cc-pVDZ++ pole strengths. The interested reader is referred to several works by our group [17,36–39] for an assessment of the approach against experimental results by the EMS research group at Beijing university.

All DFT calculations described in the present work have been performed using the GAUSSIAN03 package of programs [40], using the default fine integration grid, which consists of 75 radial shells and 302 angular points per shell resulting in about 7000 points per atom. Lacking the original numerical data, experimental (e,2e) ionization cross sections were obtained by digitizing the experimentally momentum distributions presented in [1] as a function of the target electron momentum, by means of the so-called 'GetData Graph Digitizer' package [41].

3. Results and discussion

Inspection of Figure 1, and comparison of the ADC(3)/6-31G, ADC(3)/cc-pVDZ, and ADC(3)/cc-pVDZ++ ionization spectra therein confirm readily the overall limited influence of the basis set upon relative ionization energies, including shake-up ionization energies, as well as on convoluted spectral envelopes, and this up to the vertical double ionization (VDI) threshold, which benchmark calculations employing Coupled Cluster theory with Single, Double and perturbative Triple excitations [CCSD(T)] [42] and the aug-cc-pVTZ basis set locate at ~26.5 eV.

The reader is referred to Table 1 and Figure 2 for a comparison with the available photoelectron and (e,2e) ionization spectra. All bands (**A**–**K**) that emerge in these measurements are in clear one-to-one correspondence with our simulations. As usual [43–46], improving the basis set results merely into a redistribution of the shake-up ionization intensity over more and more satellites (Fig. 1), but without qualitatively any significant change in the

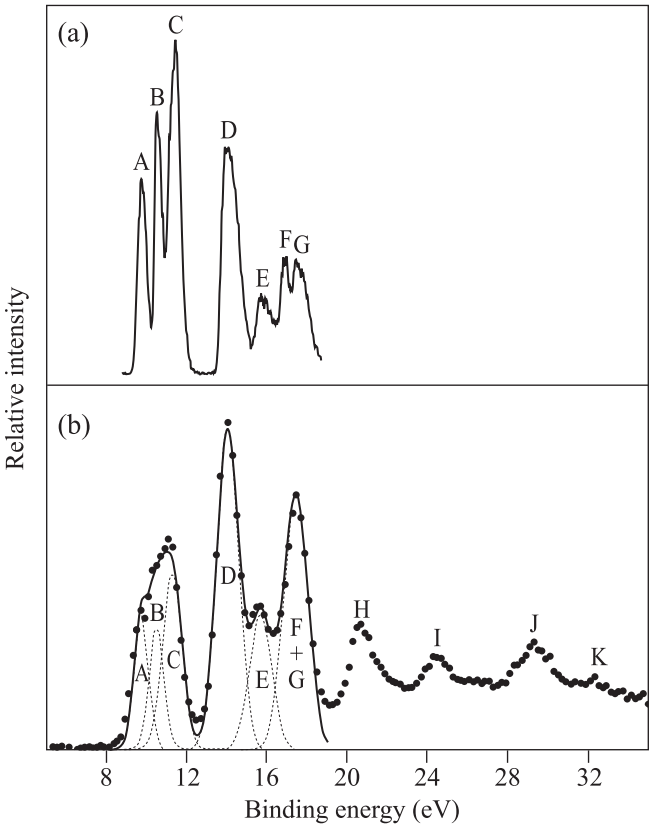

Figure 2. Experimental ionization spectra of pyrimidine ($C_4N_2H_4$, C_{2v} symmetry point group): (a) photoelectron spectrum ($h\nu = 45$ eV) [5]; and (b) integrated (e,2e) ionization spectrum ($E_0 = 1.5$ keV) [1]. See Table 1 for a detailed assignment of lines and bands.

shape and orbital assignment of spectral bands. The influence of the basis set increases beyond the VDI threshold, where the computed shake-up states are nothing more than approximations to shake-off resonances embedded in the continuum. The comparison of the three ADC(3) spectra in Figure 1 confirms that the 6–31G basis set is amply sufficient for correctly assigning the valence ionization spectrum of pyrimidine. We note in particular that, if the basis set appears to have quantitatively a quite significant influence on the $2b_1^{-1}$ one-electron ionization energy, a trend which larger scale OVGF calculations confirm, its influence on the associated pole strength remains marginal (Table 1).

The shake-up onset is located at 14.9 eV. It corresponds to a rather intense satellite [$\Gamma = 0.09$] of the $10a_1$ orbital that relates

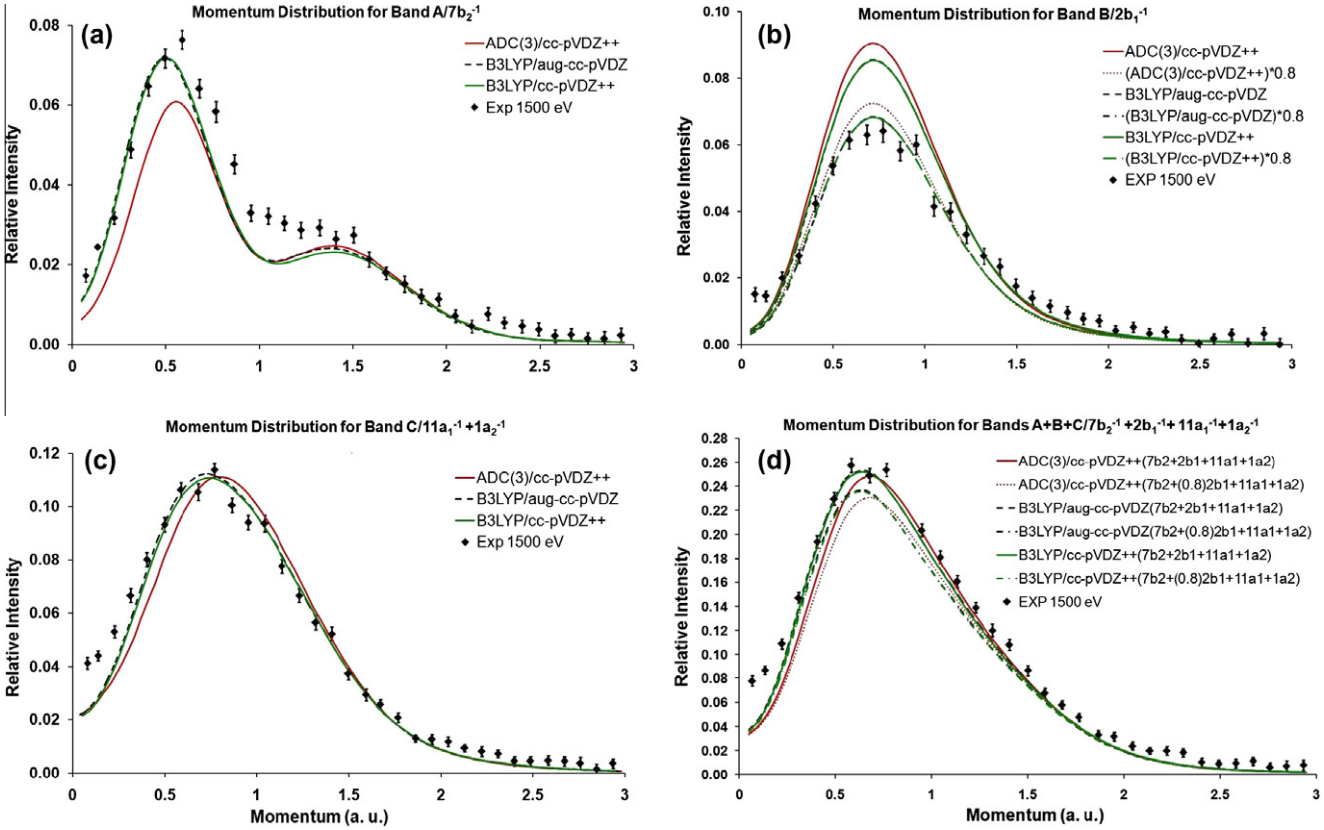

Figure 3. Comparison between experimental and theoretical electron momentum distributions inferred at an electron impact energy of 1.5 keV for the four outermost ionization lines, at binding energies below 12 eV. Experimental momentum distributions were taken from the work by Ning et al. in Ref. [1], prior to a global rescaling onto our most thorough (many-body) ADC(3) results.

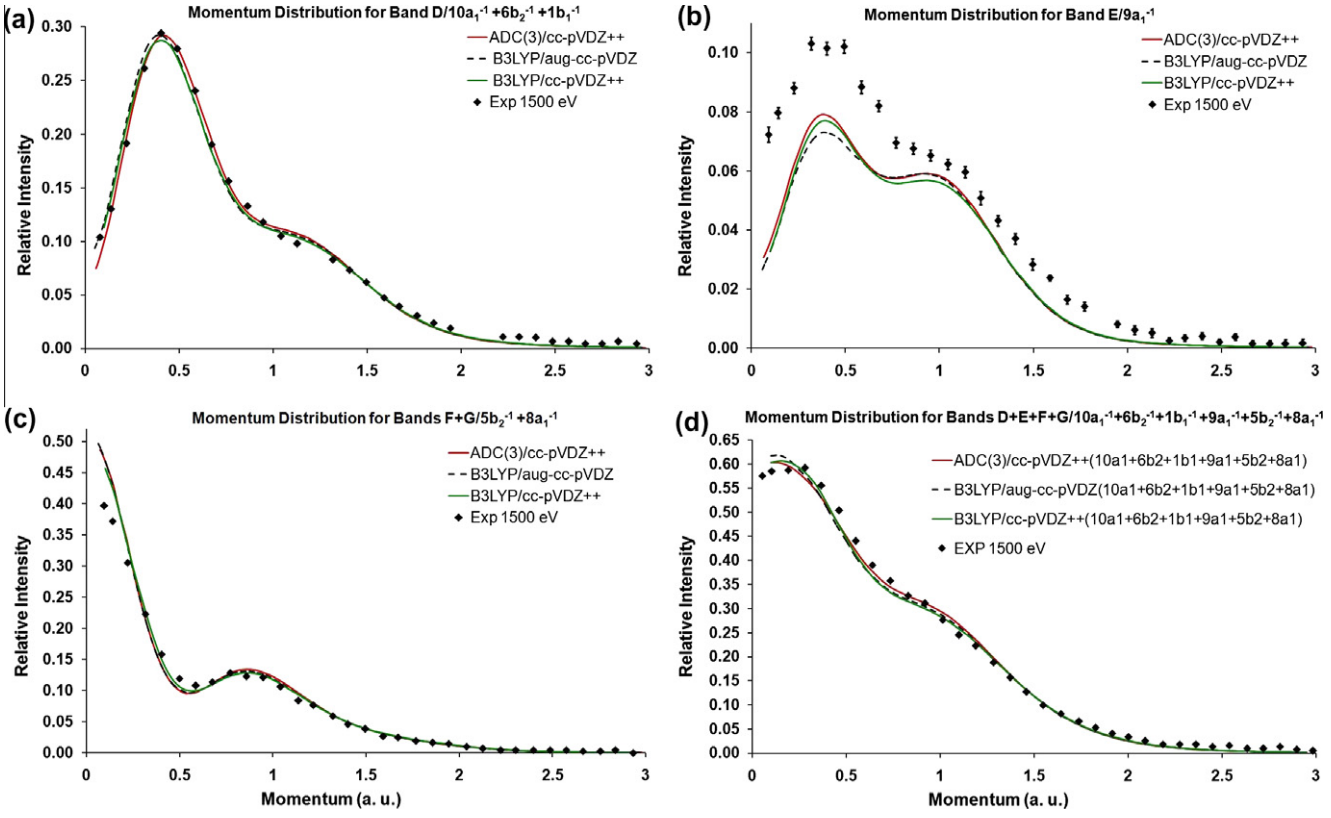

Figure 4. Comparison between experimental and theoretical electron momentum distributions inferred at an electron impact energy of 1.5 keV for ionization lines, at binding energies comprised between 12 and 19 eV. Experimental momentum distributions were taken from the work by Ning et al. [1], prior to a global rescaling onto our most thorough (many-body) ADC(3) results.

dominantly to the $2h\text{-}1p$ $7b_2^{-1}$ $2b_1^{-1}$ $2a_2^{+1}$ electronic configuration. Whatever the basis set employed, the $5b_2$ intensity is basically shared by two ionization lines of approximately equal strength at 17.3 and 17.6 eV. The orbital picture of ionization breaks down completely at electron binding energies above 20 eV, and bands **H**, **I**, **J**, and **K** at ~21, ~24 ~29 and ~32 eV in the (e,2e) ionization spectrum (Fig. 2b) can be safely ascribed to $\{7a_1 + 4b_2\}$, $6a_1$, $3b_2$, and $5a_1$ shake-up satellites and/or shake-off resonances (beyond the VDI threshold), respectively. Except for the energy interval between the two first ionization lines (bands **A** and **B**), all our ADC(3) data entirely corroborate the assignment proposed by Potts et al. [5].

In straightforward analogy with the text book example given by N_2 [47], an inversion of the order predicted on the ground of Koopmans' theorem (KT) for the first two lines is observed when electronic correlation and relaxation are taken into account, the nitrogen lone pair orbitals (e.g. $7b_2$) being inherently subject to stronger orbital and pair relaxation (ORX < 0, PRX < 0) corrections [47] to ionization energies, whereas π-orbitals (e.g. $2b_1$) most usually produce stronger pair removal (PRM > 0) corrections [47]. Larger basis sets are obviously required for quantitatively describing electronic relaxation processes towards localized hole states in a strongly polarized environment. Noticeable differences in shifts in electron binding energies are indeed observed for the $7b_2$ and $2b_1$ orbitals,+0.56 versus +0.11 eV, respectively, when replacing the 6–31G basis set by the cc-pVDZ++ one. As far as can be judged from the relative position of this orbital in the photoelectron spectrum (Fig. 2a) compared with the trends emerging from ADC(3) simulations employing basis sets of improving quality (Fig. 1), strong geometrical relaxation and vibronic complications are likely to interfere upon removal of an electron from the $7b_2$ nitrogen lone-pair level, in which case the position of the corresponding maximum in intensity may in turn deviate by a few tenths eV from the vertical estimate. Note also that (e,2e) ionization processes at large electron impact energies (1.5 keV) and photoelectron experiments at rather low photon energies (40–80 eV) may occur on significantly different timescales. The greatest care is therefore required upon analyzing separately the electron momentum distributions corresponding to the three outermost ionization bands (**A**–**C**) in the EMS spectrum, experimentally located at energy intervals (~0.70 eV) that dangerously coincide with the retained value of 0.68 eV (FWHM) for the experimental resolution [1].

Following the analysis by Ning et al. [1], we compare in Figures 3 and 4 our theoretical results with the experimental momentum distributions inferred from an angular analysis of the (e,2e) ionization intensities characterizing bands **A**–**C** and **D**–**G**, respectively, based on the following assignment: **A** = $7b_2^{-1}$; **B** = $2b_1^{-1}$; **C**=$\{11a_1^{-1} + 1a_2^{-1}\}$; **D**=$\{10a_1^{-1} + 6b_2^{-1} + 1b_1^{-1}\}$; **E** = $9a_1^{-1}$; {**F** + **G**}=$\{5b_2^{-1} + 8a_1^{-1}\}$. In view of the importance of relaxation effects upon electron removal from strongly localized nitrogen lone pairs, it is not entirely a surprise to observe (Fig. 3a and c) significant differences between ADC(3) Dyson and B3LYP Kohn–Sham orbital momentum distributions for the $7b_2^{-1}$ and $11a_1^{-1}$ one-electron ionization lines. A significant re-localization of the electron densities towards the nitrogen lone pair region is correspondingly noticed when comparing (correlated and relaxed) ADC(3) Dyson to (correlated but unrelaxed) B3LYP Kohn–Sham orbital densities for the two lone-pair levels (Fig. 5e and h). In contrast (Fig. 3b and c), the π-ionization lines ($2b_1$, $1a_2$) produce ADC(3) Dyson and B3LYP Kohn–Sham orbital momentum distributions that are essentially similar, and comparing ADC(3) Dyson to B3LYP Kohn–Sham orbital densities in this case indicate merely a re-localization of π-densities away from the nitrogen atoms (Fig. 5f and e). Plots of density differences between ADC(3) Dyson and HF orbitals (Fitures 5a–d), on the one hand, and ADC(3) Dyson and KS orbitals (Fig. 5e–h), on the other hand, indicate usually opposite charge reorganizations. This observation is in line with the view that if they (empirically) account for ground state electron correlation, standard B3LYP Kohn–Sham orbitals do not account for electronic relaxation. Passing by, we note that B3LYP Kohn–Sham electron momentum distributions obtained using the closely related aug-cc-pVDZ and cc-pVDZ++ basis sets are almost identical.

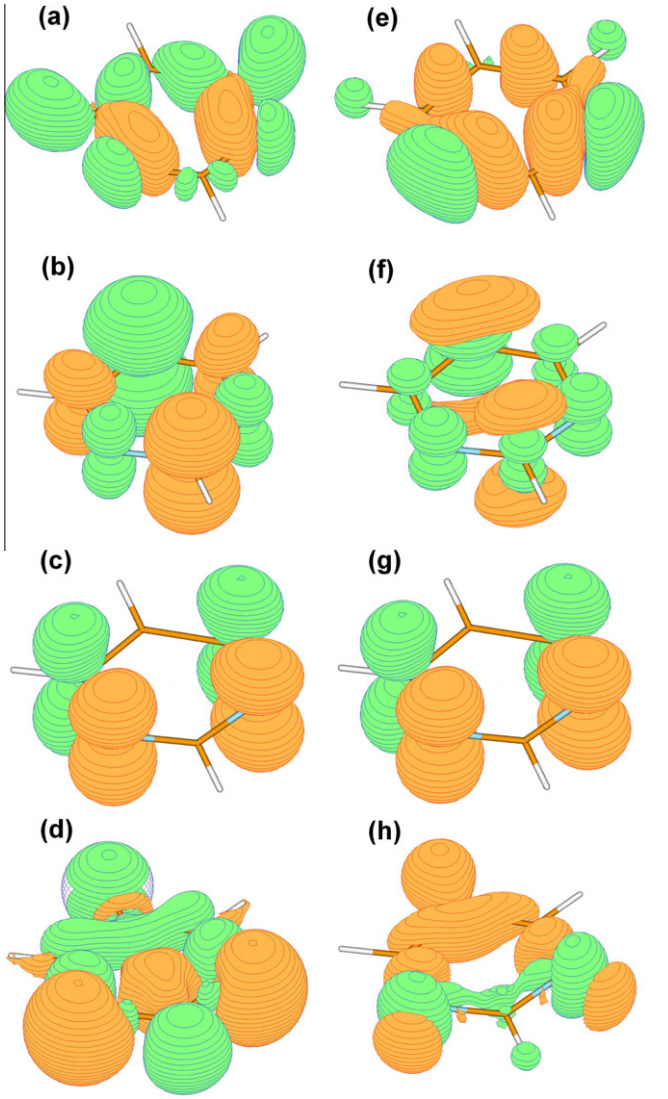

Figure 5. Contour plots of electron density differences ($\Delta\rho$) between normalized averaged Dyson orbitals and the related HF orbitals (left) or KS orbitals (right) – see [37] for detailed explanations about the procedure followed to compute these plots (all results were obtained using the cc-pVDZ++ basis set). The selected values for the contours are 0.0005. The green and yellow areas correspond to regions that exhibit an increase or decrease of the electron density, respectively. (For interpretation of the references to colour in this figure legend, the reader is referred to the web version of this article.)

As was noted in [1], a best fit between theory and experiment is possible for the $2b_1^{-1}$ state alone when multiplying the computed momentum distributions by a factor ~0.8 (Fig. 3b). Whatever the employed basis set, this rescaling is obviously not supported at the ADC(3) level. It is clearly the result of strong overlap effects between bands **A**–**C**: when considering summed momentum distributions for these three bands, the best agreement between theory and experiment is overall unquestionably obtained (Fig. 3d) when using the full $2b_1^{-1}$ contribution to the global momentum profile. In view of the underlying d-like orbital topology (two perpendicular nodal

planes), marginal turn-ups of the experimental (e,2e) ionization intensities at low momenta for the $2b_1$ momentum profile (Fig. 3b) may be ascribed to distorted wave effects.

At larger binding energies (Fig. 4), ADC(3) Dyson and B3LYP Kohn–Sham orbitals produce essentially equivalent momentum profiles, and the agreement with experiment is overall qualitatively more than satisfactory. A rather substantial discrepancy with theoretical results for band E (Fig. 4b) is again to be ascribed to an improper treatment of overlap effects in the original work by Ning et al. [1]. Indeed, when considering the photoelectron spectrum displayed in Figure 2a, it is clear that the adjacent band D is subject to enhanced vibrational broadening. Also, there is a perfect match between theory and experiment when considering summed electron momentum distributions for bands D + E + F + G (Fig. 4d).

4. Conclusions

A thorough theoretical study of the electronic structure, ionization spectrum and electron momentum distributions of pyrimidine has been presented, on the ground of 1p-GF/ADC(3) calculations of one-electron and shake-up ionization energies and of the related Dyson orbitals, and a comparison with available photoelectron and EMS experiments. Quantitative agreement is found between the UPS and EMS electron binding energies, on the one hand, and the results of large scale 1p-GF (OVGF, ADC(3)) calculations, on the other hand. ADC(3) pole strengths are found to be quantitatively consistent with the experimental (e,2e) ionization intensities and the correspondingly inferred orbital momentum distributions, provided severe band overlaps among the outermost valence bands are correctly accounted for in the analysis: all four outermost ionization lines exhibit essentially equal ADC(3) pole strengths ($\sim$0.89), and there is no need to rescale the $2b_1$ intensities for consistently interpreting the outermost momentum distributions. Again, we would like to advocate 1p-GF/ADC(3) theory for interpreting EMS experiments, as one of the most accurate and nowadays most commonly accepted standards for computations of vertical one-electron and shake-up ionization spectra. We have also to remind that risks are inherent to any spectral analysis that lies at the confines of, or goes beyond the permitted energy resolution.

Acknowledgments

All calculations presented in this work have been performed on a Compaq ES47 work station at Hasselt University, Belgium. This work has been supported by the FWO-Vlaanderen, the Flemish branch of the Belgian National Science Foundation, and by the BijzonderOnderzoeksFonds (BOF: special research fund) at Hasselt University. M. S. D and B. H. especially acknowledge financial support from a Research Program of the Research Foundation - Flanders (FWO_Vlaanderen; project number G.0350.09 N, entitled '*From orbital imaging to quantum similarity in momentum space*'.

References

[1] C.G. Ning, K. Liu, Z.H. Luo, S.F. Zhang, J.K. Deng, Chem. Phys. Lett. 476 (2009) 157.
[2] I.E. McCarthy, E. Weigold, Rep. Prog. Phys. 54 (1991) 789.
[3] M.A. Coplan, J.H. Moore, J.-P. Doering, Rev. Mod. Phys. 66 (1994) 985.
[4] E. Weigold, I.E. McCarthy, Electron Momentum Spectroscopy, Kluwer Academic Plenum Publishers, New York, 1999.
[5] A.W. Potts, D.M.P. Holland, A.B. Trofimov, J. Schirmer, L. Karlsson, K. Siegbahn, J. Phys. B: At. Mol. Opt. Phys. 36 (2003) 3129.
[6] B.T. Pickup, O. Goscinski, Mol. Phys. 26 (1973) 1013.
[7] L.S. Cederbaum, G. Hohlneicher, W. von Niessen, Mol. Phys. 26 (1973) 1405.
[8] L.S. Cederbaum, W. Domcke, Adv. Chem. Phys. 36 (1977) 205.
[9] W. von Niessen, J. Schirmer, L.S. Cederbaum, Comput. Phys. Rep. 1 (1984) 57.
[10] J. Schirmer, L.S. Cederbaum, O. Walter, Phys. Rev. A 28 (1983) 1237.
[11] J. Schirmer, G. Angonoa, J. Chem. Phys. 91 (1989) 1754.
[12] H.-G. Weikert, H.-D. Meyer, L.S. Cederbaum, F. Tarantelli, J. Chem. Phys. 104 (1996) 7122.
[13] M.S. Deleuze, M.G. Giuffreda, J.-P. François, L.S. Cederbaum, J. Chem. Phys. 111 (1999) 5851.
[14] Z.J. Li, X.J. Chen, X. Shan, T. Liu, K.Z. Xu, J. Chem. Phys. 130 (2009) 054302.
[15] P. Duffy, D.P. Chong, M.E. Casida, D.R. Salahub, Phys. Rev. A 50 (1994) 4707.
[16] W.J. Hehre, R. Ditchfield, J.A. Pople, J. Chem. Phys. 56 (1972) 2257.
[17] C.G. Ning et al., Chem. Phys. 343 (2008) 19.
[18] L.S. Cederbaum, W. Domcke, J. Schirmer, W. von Niessen, Adv. Chem. Phys. 65 (1986) 115.
[19] M.S. Deleuze, Chem. Phys. 329 (2006) 22.
[20] A.B. Trofimov, J. Schirmer, V.B. Kobychev, A.W. Potts, D.M.P. Holland, L. Karlsson, J. Phys. B 39 (2006) 305.
[21] V.G. Zakrzewski, O. Dolgounitcheva, J.V. Ortiz, J. Chem. Phys. 129 (2008) 104306.
[22] M.S. Deleuze, S. Knippenberg, J. Chem. Phys. 125 (2006) 104309.
[23] R.G. Parr, W. Yang, Density Functional Theory of Atoms and Molecules, Oxford University Press, New York, 1989.
[24] (a) A.D. Becke, J. Chem. Phys. 98 (1993) 5648;
(b) C. Lee, W. Yang, R.G. Parr, Phys. Rev. B 37 (1988) 785.
[25] T.H. Dunning Jr., J. Chem. Phys. 90 (1989) 1007.
[26] R.A. Kendall, T.H. Dunning Jr., R.J. Harrison, J. Chem. Phys. 96 (1992) 6796.
[27] The original ADC(3) code by G. Angonoa, O. Walter, J. Schirmer; further developed in its version named 'AGAMIP' by M.K. Scheller; contributions due to A.B. Trofimov.
[28] M.W. Schmidt et al., QCPE Bull. 10 (1990) 52.
[29] M.S. Deleuze, Int. J. Quantum Chem. 93 (2003) 191.
[30] A. Ruhe, Math. Comput. 33 (1979) 680.
[31] H.-D. Meyer, S. Pal, J. Chem. Phys. 91 (1989) 6195.
[32] F. Tarantelli, A. Sgamellotti, L.S. Cederbaum, J. Schirmer, J. Chem. Phys. 86 (1987) 2201.
[33] See various contributions to the original HEMS program as recorded by Bawagan [A.O. Bawagan, Ph. D. Thesis, University of British Columbia (UBC), 1987]. The HEMS (now known as MOMAP) program has been extensively revised and extended at UBC by N.M. Cann and G. Cooper.
[34] X.G. Ren, C.G. Ning, J.K. Deng, S.F. Zhang, G.L. Su, F. Huang, G.Q. Li, Rev. Sci. Instrum. 76 (2005) 063103.
[35] P. Duffy, M.E. Casida, C.E. Brion, D.P. Chong, Chem. Phys. 159 (1992) 347.
[36] C.G. Ning, X.G. Ren, J.K. Deng, G.L. Su, S.F. Zhang, S. Knippenberg, M.S. Deleuze, Chem. Phys. Lett. 421 (2006) 52.
[37] Y.R. Huang et al., J. Phys. Chem. A 112 (2008) 2339.
[38] Y.R. Huang, C.G. Ning, J.K. Deng, M.S. Deleuze, Phys. Chem. Chem. Phys. 10 (2008) 2374.
[39] F. Morini, B. Hajgató, M.S. Deleuze, C.G. Ning, J.K. Deng, J. Phys. Chem. A 112 (2008) 9083.
[40] M.J. Frisch et al., GAUSSIAN03, Revision D.01, Gaussian Inc., Pittsburgh, PA, 2003.
[41] See http://getdata-graph-digitizer.com/.
[42] G.D. Purvis, R.J. Bartlett, J. Chem. Phys. 76 (1982) 1910.
[43] M.S. Deleuze, A.B. Trofimov, L.S. Cederbaum, J. Chem. Phys. 115 (2001) 5859.
[44] M.S. Deleuze, J. Chem. Phys. 116 (2002) 7012.
[45] M.S. Deleuze, J. Phys. Chem. A 108 (2004) 9244.
[46] N. Kishimoto, Y. Hagihara, K. Ohno, S. Knippenberg, J.-P. François, J. Phys. Chem. A 109 (2005) 10535.
[47] A. Szabo, N.S. Ostlund, Modern quantum chemistry, Introduction To Advanced Electronic structure Theory, McGraw Hill, New York, 1989.